

Structure of Platinum Particles Deposited on Titanium Dioxide (110) Surface Studied by X-Ray Photoelectron Diffraction

Koji TAMURA,* Masanori OWARI, and Yoshimasa NIHEI

Institute of Industrial Science, University of Tokyo,

7-22-1 Roppongi, Minato-ku, Tokyo 106

(Received October 9, 1987)

Platinum atoms deposited on a TiO_2 (110) surface were studied by X-ray photoelectron diffraction, and the structure of the platinum particles was clarified. It was found that after annealing at 823 K for 30 min the platinum particles coalesced and that the structural model of platinum particles based on the (111) surface of the fcc crystal explained the experimental XPED patterns very well.

Small metal particles are an interesting subject in the field of chemistry and physics.¹⁾ Especially, the structure and the chemical state of noble metal particles on metal oxides are important in connection with supported metal catalysts.^{2,3)}

In general, in order to obtain structural information about small metal particles, transmission electron microscopy (TEM) or extended X-ray absorption fine structure (EXAFS) have been used. In order to obtain a TEM micrograph or microdiffraction pattern, the irradiation of small metal particles by an electron beam is essential. However, the damage caused by the high energy electron beam is serious. Iijima has studied ultrafine particles of gold by electron microscopy, and emphasized that the structure of the gold particles became unstable because of charge fluctuations when they were exposed to intense electron-beam irradiation.⁴⁾ It is also difficult for TEM measurement to use a well defined single crystal sample as a support. From EXAFS measurements, information on the surrounding atoms about a particular type of atom is obtained such as the number of neighboring atoms and their distance from the reference atom. This information is, however, insufficient to create a three dimensional structural model or determine the directional relation between overlayer and substrate.

X-Ray photoelectron diffraction (XPED) has been shown to be a promising new method for surface structural and chemical state analysis,^{5,6)} and does not have these drawbacks. The advantages of XPED measurement compared with other surface analytical methods are summarized as follows: 1) the charging of a sample does not prevent obtaining clear diffraction patterns; 2) long-range ordering is not necessary to obtain structural information; 3) the contribution as an emitter atom from each component can be distinguished. From these features, XPED measurement is considered to be a more desirable method to analyze the metal particles deposited on insulating materials like metal oxides than other conventional methods. Kudo et al. have applied XPED measurement to gold atoms evaporated on a semiconductor, namely, GaAs(110), (001), Ge(110), and GaSb(110),

and characterized the surface layer of metal-semiconductor contacts.⁷⁾

In this study, the XPED patterns for platinum atoms deposited on a TiO_2 (110) surface were obtained, and the structure of the platinum particles was analyzed by a theoretical calculation. This sample was studied as a well-defined model system of Pt/ TiO_2 catalyst which is one of the most important systems among supported metal catalysts. When one attempts to explain catalysis, the phenomenon becomes ambiguous for practical catalysts, because of uncertainty about the impurities, or atomic structure of the substrate etc. To clarify the essential nature of catalysis, the investigation of model catalysts is very useful.

Experimental

All experiments were performed with an angle-resolved X-ray photoelectron spectrometer, which was equipped with a hemi-spherical electron energy analyzer and computer controlled multichannel detection system.⁸⁾ Aluminum $K\alpha$ radiation was used to excite photoelectrons. The base pressure of the system was less than 2.7×10^{-8} Pa.

A (110) oriented TiO_2 rutile single crystal, obtained from the Nakazumi Crystal Laboratory, was aligned to within $\pm 0.5^\circ$ of the desired orientation. This was checked by the Laue back reflection. The crystal was then mechanically polished, and chemically etched. Before measurements, the sample was cleaned by Ar^+ -ion bombardment (700 eV) and annealing (1010 K) cycles. The temperature was monitored with a chromel-alumel thermocouple spotwelded to the sample holder. Since oxygen atoms diffused out from the bulk of the sample because of the annealing treatment, the surface stoichiometry change caused by the selective sputtering was sufficiently restored. This was checked from the shape of $\text{Ti}2p$ spectra and the valence spectra. The cleanliness of substrate surface was checked by X-ray photoelectron spectroscopy, and no carbon nor other impurities were detected.

The platinum was evaporated in vacuum by resistively heating from a pure platinum ribbon onto the titanium dioxide. The deposition rate of platinum was approximately $0.08 \text{ \AA min}^{-1}$. To eliminate the apparent shift caused by the charging of the sample, the binding energy of platinum 4f was calibrated from the $\text{Ti}2p_{3/2}$ peak (458.8 eV).

Results and Discussion

The azimuthal dependences of Ti2p emission from TiO₂ (110) at a polar angle $\theta=50^\circ$ relative to the surface normal are shown in Fig.1(a). The XPED pattern exhibited much fine structure, which indicated that the crystal regularity was sufficiently restored after the annealing treatment. The XPED pattern was mirror symmetric about the azimuthal angle $\phi=0^\circ$ ([1 $\bar{1}$ 0] direction of TiO₂) and 90° ([001] direction), which reflected the crystal structure. Though it was impossible to obtain full 360° azimuthal dependences by one scan with our system, different part of the azimuthal dependences which are not shown in this figure was checked by another

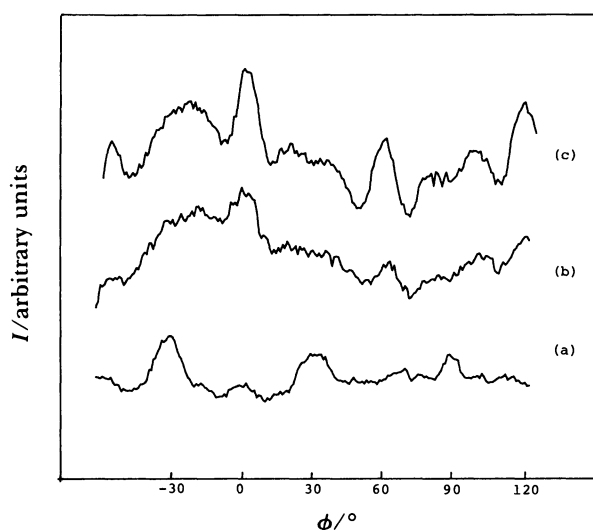


Fig. 1. (a) Azimuthal pattern of Ti2p at $\theta=50^\circ$ from TiO₂(110). (b) Azimuthal pattern of Pt4f at $\theta=53^\circ$ deposited on TiO₂(110) to a thickness of about 15.8 Å. (c) Azimuthal pattern of Pt4f at $\theta=53^\circ$ after annealing at 823 K for 30 min.
 ϕ : Azimuthal angle. I : Intensity.

experiment. These results indicated that the XPED pattern of TiO₂(110) has two-fold symmetry.

Figure 2 shows the XPS signal intensity (a) and the binding energy (b) of the Pt4f level as a function of the metal coverage. It was evident from these results that the binding energy of Pt4f_{7/2} level decreased as the metal coverage increased. The decrease of the binding energy was caused mainly by the change of the degree of the screening of a core-hole by the electrons of

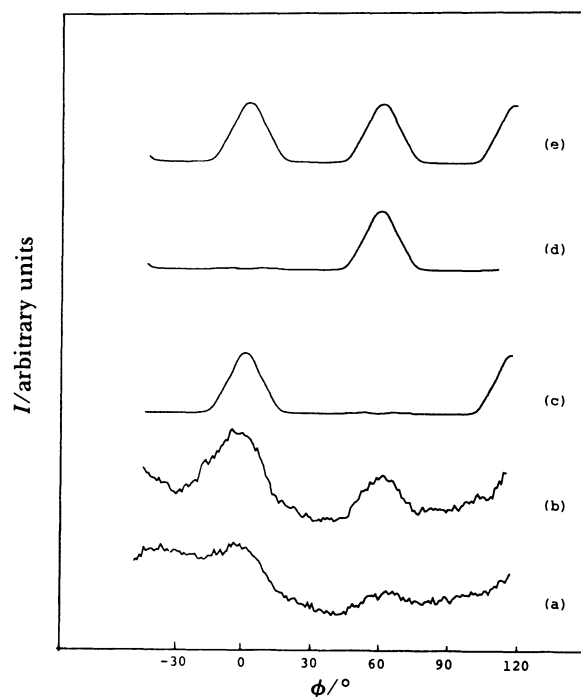


Fig. 3. (a) Azimuthal pattern of Pt4f at $\theta=33^\circ$ deposited on TiO₂(110) to a thickness of about 15.8 Å. (b) Azimuthal pattern of Pt4f at $\theta=33^\circ$ after annealing at 823 K for 30 min. (c) Calculated pattern of Pt4f from platinum No. 1. (d) Calculated pattern from platinum No. 2. (e) Calculated pattern when two types of particles exist.

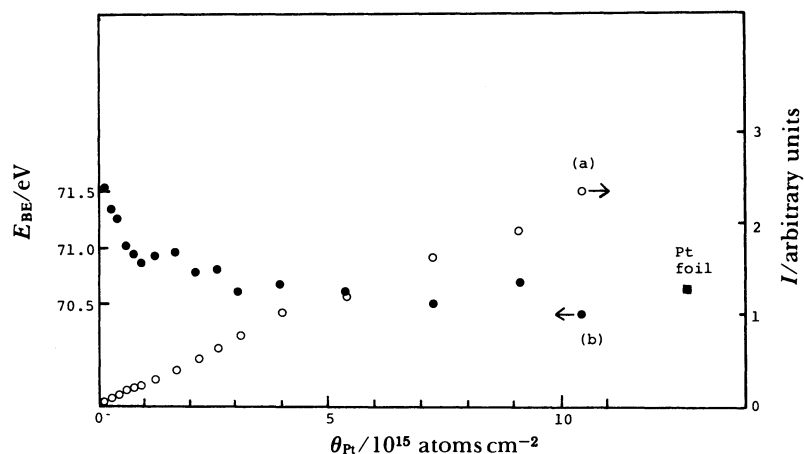


Fig. 2. (a) XPS signal intensity of Pt4f. (b) Binding energy of Pt4f_{7/2} as a function of Pt coverage.
 θ_{Pt} : Pt coverage. E_{BE} : Binding energy.

neighboring atoms.³⁾ In larger particles, since there were more neighboring electrons, the screening was more effective than in smaller particles, and the binding energy lowered. The amount of platinum deposited after the final step of the deposition was equivalent to the layer 15.8 Å in thickness, if layer growth was assumed. This thickness was roughly estimated from the XPS signal intensity ratio of Pt4f peak to Ti2p peaks assuming that the mean free path is 20 Å. XPED patterns were measured at this final point.

The azimuthal dependences of Pt4f emission at polar angles $\theta=53^\circ$ (Fig. 1(b)) and $\theta=33^\circ$ (Fig. 3(a)) just after deposition were obtained. As can be seen in these XPED patterns, the photoelectron intensity maxima were already observed at $\phi=0^\circ, 60^\circ, 120^\circ$, which indicated that the platinum had structural regularity to some degree.

The sample was then annealed at 823 K for 30 min, which caused some significant changes. First, the XPS intensities for titanium and oxygen atoms relative to platinum atoms increased. Thus, the average thickness of the platinum, determined from the XPS signal intensity ratio, decreased to 7.6 Å. Second, as shown in Fig. 1 (c) for $\theta=53^\circ$ and Fig. 3 (b) for $\theta=33^\circ$, the modulation of the XPED patterns increased and the patterns became clear. The amplitude of the anisotropy, defined as the ratio of (maximum–minimum)/maximum for $\theta=53^\circ$ (Fig. 1 (b), (c)), increased from 16% to 29%. In contrast to the pattern from the titanium atom (Fig. 1 (a)), these patterns can be regarded as having six-fold symmetry rather than two-fold symmetry.

These results indicated that most of platinum particles coalesced and became larger (metal agglomeration) on heat treatment, and simultaneously the degree of crystallization of the Pt particles and the degree of epitaxial relation between overlayer and substrate increased. Since the exposed area of the substrate surface increased on coalescence of the platinum particles, the XPS intensity from the substrate increased. On the other hand, since the exposed surface area of the platinum particles decreased on coalescence, the intensity from overlayer

decreased. As a result, the Pt/Ti signal ratio decreased.

The diffusion of platinum atoms into the substrate may also decrease the Pt/Ti signal ratio, but this contribution was not so large, because 1) the chemical state of the platinum atom in the substrate must be different from that on the substrate, and these differences must be reflected in the platinum spectra. But no significant changes were observed in the platinum 4f spectral region. 2) if platinum atoms diffused into the substrate, the XPED pattern shows two-fold symmetry (selective incorporation case) or smaller modulation (random incorporation case), which were different from the experimental observation.

Assuming the coalescence is due to annealing only, the degree of coalescence could be estimated roughly based on a simple model as follows. The model is shown in Fig. 4 (a),(b). Hemi-spherical particles were assumed on the basis of the experimental observation by electron microscopy that the platinum particles grew in an island-like fashion on TiO_2 .⁹⁾ The highly dispersed particles (a) just after deposition coalesced and became larger particles (b) because of annealing. Based on this model, the XPS signal intensity of the platinum atom for normal exit angle after annealing was written as

$$I_{\text{Pt}} = 2\pi I_{\text{Pt}}^\infty \left[\frac{1}{2} N^{2/3} a^2 - \int_0^{N^{1/3}a} r \cdot \exp(-\sqrt{N^{2/3}a^2 - r^2}/\lambda) dr \right]. \quad (1)$$

The XPS intensity of the titanium atom in the exposed substrate was written as

$$I_{\text{Ti}}(1) = I_{\text{Ti}}^\infty (2\sqrt{3}N - \pi N^{2/3}) a^2, \quad (2)$$

and the intensity of the titanium under the platinum particle was

$$I_{\text{Ti}}(2) = 2\pi I_{\text{Ti}}^\infty \left[\int_0^{N^{1/3}a} r \cdot \exp(-\sqrt{N^{2/3}a^2 - r^2}/\lambda) dr \right], \quad (3)$$

where I_{Pt}^∞ and I_{Ti}^∞ were the XPS intensities of platinum and titanium from a semi-infinite platinum and TiO_2 layer, respectively; λ was the attenuation length, and a

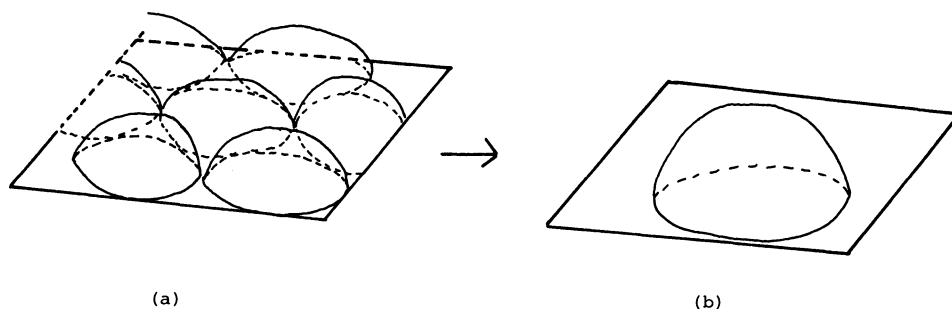


Fig. 4. Schematic representation of platinum particles on $\text{TiO}_2(110)$ (a) just after deposition and (b) after annealing at 823 K for 30 min.

the radius of a particle just after deposition. N was the number of particles which gathered and became one larger particle because of the annealing treatment. Thus, the relative intensity of Pt to Ti after annealing became $(1)/((2)+(3))$, and the degree of coalescence N could be determined from the experimental signal ratio. It was estimated from the experimental XPS data that because of the heat treatment the volume of a particle increased about 26 times, and the exposed surface area of the platinum particles decreased to about 34% of that before annealing.

Ocal et al. have observed that annealing at 800 K in vacuum, which was almost the same treatment as our study, caused the suppression of CO adsorption for a Pt/TiO₂ sample and the uptake of CO per Pt atom was reduced by a factor of 2.¹⁰ They suggested its relation to, what is called, strong metal-support interaction (SMSI), which recently attracted much interests in the field of catalysis.¹¹ The predominant model to explain this phenomenon is called the migration or decoration model, in which, titanium sub-oxide TiO_x migrates from a substratum and covers the surface area of the dispersed metal.¹² This may also decrease the Pt/Ti signal ratio. Ocal et al. also observed the Ti³⁺ state after vacuum annealing of a Pt/TiO₂ sample at 800 K, and the relative concentration of Ti³⁺ to Ti⁴⁺ ion was about 20%.¹⁰ Greenlief et al. have observed the Ti³⁺ state after the vacuum annealing of TiO₂ overlayer on Pt at 1300 K,¹³ which was higher than our temperature. They suggested a model in which the reduced titania

species diffused into the platinum layer. Figure 5 shows the experimental spectra of Ti2p emission before platinum deposition (a) and after the annealing treatment (b). The height of these spectra was normalized and all of the spectra were smoothed. After annealing under these experimental conditions, namely, platinum deposited on TiO₂ (110) single crystal annealed in UHV at 823 K for 30 min, a small amount of a lower binding energy state did appear. But even if it covered the surface of the Pt particle because of migration, its contribution to the decrease of the Pt/Ti signal intensity ratio after the annealing was small. This indicated that the large decrease of the Pt/Ti ratio was not caused by the migration of sub-oxide onto the Pt particle.

The structural analysis of the platinum particles was next investigated by theoretical calculations. The calculations were performed within the double scattering approximation, in which the total photoelectron wave was expressed as a sum of a direct wave, a single-scattering wave and a double-scattering wave. The scattering amplitude for the double-scattering wave was a product of each scattering amplitude. Inelastic damping factors were derived from a sum of each path. Elastic scattering amplitudes were obtained from tabular form data.¹⁴ The cluster of atoms used in this calculation consisted of a hemi-spherical platinum cluster 15 Å in radius

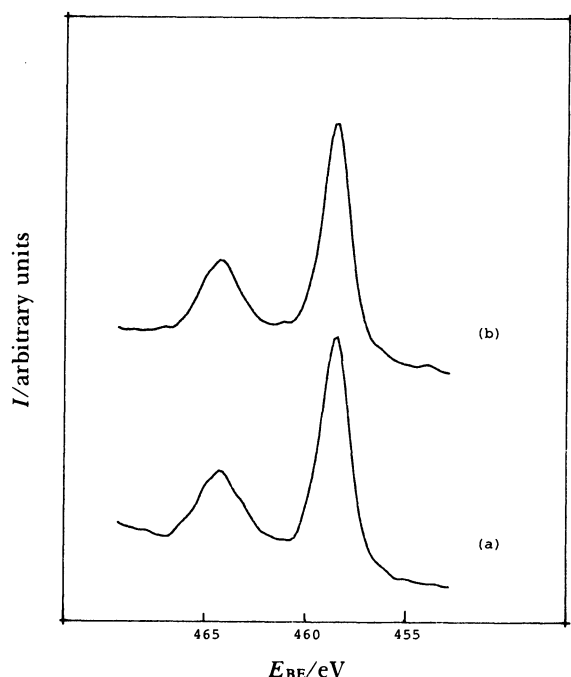


Fig. 5. XPS spectra of Ti2p from (a) clean TiO₂(110) surface and (b) Pt/TiO₂(110) annealed at 823 K for 30 min.

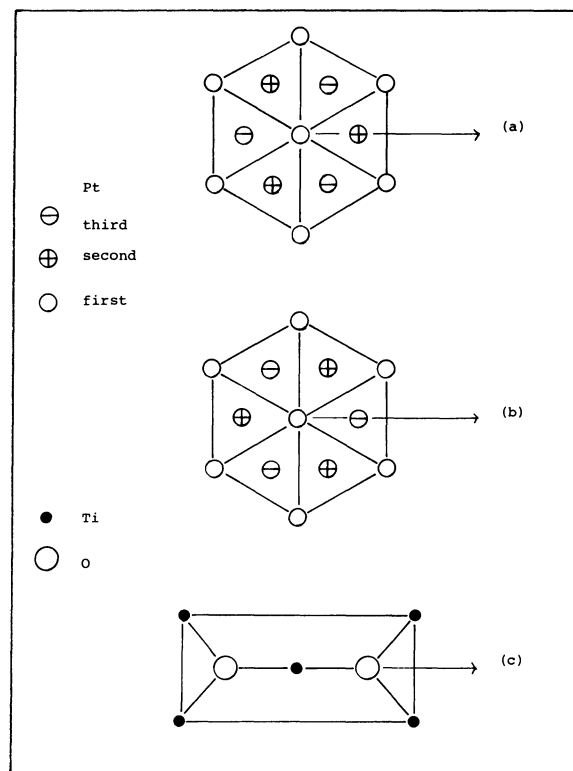


Fig. 6. (a), (b) Structural model of platinum particles No. 1 and No. 2. (c) Structural model of TiO₂(110) surface.

and a substrate cluster whose atoms were within 10 Å to the emitter atom. Since the six-fold symmetry of the experimental results was explained by the multiple of two fold-symmetry of the substrate and three-fold symmetry of the overlayer, it was sufficient to assume only the structural model based on the (111) plane of fcc platinum crystal. Two cluster models No. 1 and No. 2 were assumed and they are shown in Fig. 6(a),(b). The cluster model No. 1 is expressed as follows; (111) plane of platinum is parallel to the (110) surface of titanium dioxide (Fig. 6(c)) and $[\bar{2}11]$ direction of the former is parallel to $[1\bar{1}0]$ direction of the latter. The cluster model No. 2 is mirror symmetric with the model No. 1 about the (110) plane of the substrate. The calculated patterns obtained from model No. 1 and No. 2 are shown in Fig. 7(b) and (c), respectively, for $\theta=53^\circ$, together with corresponding experimental pattern (a). For $\theta=33^\circ$ Fig. 3(c) and (d) show the calculated patterns from model No. 1 and No. 2, respectively. These platinum patterns were three-fold symmetric and did not agree with the experimental pattern. These two models were equivalent from the standpoint of the structural relationships between substrate and overlayer. When two clusters exist with equal probability on the surface of titanium dioxide, corresponding patterns were obtained as shown in Fig. 7(d) for $\theta=53^\circ$ and Fig. 3(e) for $\theta=33^\circ$. From the comparison, it was found that the calculated patterns at $\theta=53^\circ$ and $\theta=33^\circ$ agreed well with the experimental pattern. This model also explained other experimental results very well which were obtained by the different angular scans. Since the XPED pattern is sensitive to the crystal structure, it was concluded from the XPED analysis that after the platinum deposition the two orientations of clusters based on the (111) surface of the fcc crystal existed with equal probability on the $\text{TiO}_2(110)$ surface.

The amplitude of the anisotropy for the calculated pattern for $\theta=53^\circ$ was 96%, and was much larger than that of the experimental pattern. This deviation was explained as follows. First, in this calculation, thermal vibration of the platinum lattice was neglected. Second, emitter atoms were assumed to exist only in the center of the cluster. As a result, the contributions from the platinum atoms, which existed in the near surface region of the platinum particle, were not included. Since the intensity modulation for these platinum atoms is less than that of in the center, the modulation of the calculated pattern was overestimated. On the other hand, the degree of ordering of the real platinum particles was possibly lower than that of ideal bulk crystal, which diminished the modulation of the experimental pattern.

Figure 7(e) shows the calculated pattern which involved only a single scattering of the electrons. From the comparison it was found that the agree-

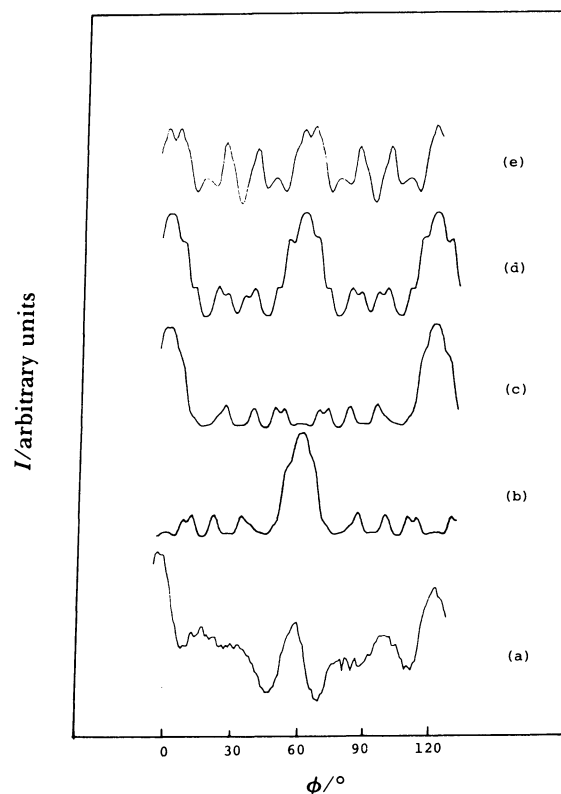


Fig. 7. (a) Azimuthal pattern of Pt4f at $\theta=53^\circ$ after annealing at 823 K for 30 min. (b) Calculated pattern from platinum No. 1 considering double scattering. (c) Calculated pattern from platinum No. 2. (d) Calculated pattern when two types of particles exist. (e) Calculated pattern considering only single scattering.

ment of the pattern was worse and the double scattering was proved to be more accurate.

Wang et al. have observed by transmission electron microscopy (TEM) that Pt particles on SiO_2 were produced with predominantly (100) and (110) planes if grown and treated in H_2 , contrary to the prospect from surface free energy.¹⁵ Our experimental results, however, showed that, when annealed in UHV, the (111) plane was the most favored, as expected for an ideal surface structure of a fcc crystal. Since the modulation of the XPED pattern of platinum after annealing was large, the contributions from the different structural particles or randomly oriented particles were small, and the structure of most of the particles was expressed by the model shown in Fig. 6. Also, the dynamic movement of the platinum particles, such as gold particles under the TEM observation, did not occur, because clear XPED patterns could not be obtained from the unstable particles.

As shown above, the structure of platinum particles deposited on a $\text{TiO}_2(110)$ surface was determined by XPED measurements. Moreover, the XPED analysis proved to be a useful technique for structural analysis

of the dispersed metal particles on the metal oxide, which were very difficult to analyze by any other technique.

We thank Dr. Masahiro Kudo for his technical assistance and for useful discussion.

References

- 1) W. D. Knight, K. Clemenger, W. A. de Heer, W. A. Sounders, M. Y. Chou, and M. L. Cohen, *Phys. Rev. Lett.*, **52**, 2141 (1984); I. Katakuse, T. Ichihara, Y. Fujita, T. Matsuo, T. Sakurai, and H. Matsuda, *Int. J. Mass Spectrom. Ion Phys.*, **67**, 229 (1985).
- 2) R. T. K. Baker, E. B. Prestridge, and R. L. Garten, *J. Catal.*, **56**, 390 (1979).
- 3) T. Huizinga, H. F. J. Vant' Blik, J. C. Vis, and R. Prins, *Surf. Sci.*, **135**, 580 (1983).
- 4) S. Iijima and T. Ichihashi, *Phys. Rev. Lett.*, **56**, 616 (1986).
- 5) Y. Nihei, M. Owari, M. Kudo, and H. Kamada, *Jpn. J. Appl. Phys.*, **20**, L420 (1981); N. Koshizaki, M. Kudo, M. Owari, Y. Nihei, and H. Kamada, *ibid.*, **19**, L349 (1980); M. Kudo, N. Koshizaki, M. Owari, Y. Nihei, and H. Kamada, *Hyoumen Kagaku*, **1**, 48 (1980).
- 6) K. Tamura, M. Owari, M. Kudo, and Y. Nihei, *Bull. Chem. Soc. Jpn.*, **58**, 1873 (1985).
- 7) M. Kudo, Pei-Xun Jien, M. Owari, N. Koshizaki, H. Kamada, and Y. Nihei, *Nippon Kagaku Kaishi*, **1985**, 1223.
- 8) M. Owari, M. Kudo, and Y. Nihei, *J. Electron Spectrosc.*, **22**, 131 (1981); M. Owari, M. Kudo, Y. Nihei, and H. Kamada, *J. Electron Spectrosc. Relat. Phenom.*, **34**, 215 (1984).
- 9) H. Nakamatsu, T. Kawai, A. Koreeda and S. Kawai, *J. Chem. Soc., Faraday Trans. 1*, **82**, 527 (1985).
- 10) C. Ocal and S. Ferrer, *J. Chem. Phys.*, **84**, 6474 (1986).
- 11) S. J. Tauster, S. C. Fung and R. L. Gartern, *J. Am. Chem. Soc.*, **100**, 170 (1978).
- 12) H. R. Sadeghi, V. E. Henrich, *J. Catal.*, **87**, 279 (1984); A. J. Simoens, R. T. K. Baker, D. J. Dwyer, C. R. F. Lund, and J. R. Madon, *J. Catal.*, **86**, 359 (1984).
- 13) C. M. Greenlief, J. M. White, C. S. Ko, and R. J. Gorte, *J. Phys. Chem.*, **89**, 5025 (1985).
- 14) M. Fink and A. C. Yates, *At. Data*, **1**, 385 (1970); M. Fink and J. Ingram, *ibid.*, **4**, 129 (1972); D. Gregory and M. Fink, *At. Data Nucl. Data Tables*, **14**, 39 (1974).
- 15) T. Wang, C. Lee, and L. D. Schmidt, *Surf. Sci.*, **163**, 181 (1985).